The Signaling Adaptor Protein CD3ζ Is a Negative Regulator of Dendrite Development in Young Neurons

Stéphane J. Baudouin,*†‡ Julie Angibaud,*†‡ Gildas Loussouarn,‡§‖
Virginie Bonnamain,*†‡ Akihiro Matsuura,¶ Miyuki Kinebuchi,¶
Philippe Naveilhan,*†‡ and Hélène Boudin*†‡

INSERM, *U643 and §U915, Nantes, F44000 France; †CHU Nantes, Institut de Transplantation et de Recherche en Transplantation, Nantes, F44000 France; ‡Université de Nantes, Faculté de Médecine, Nantes, F44000 France; ‖Centre National de la Recherche Scientifique, ERL3147, F-44000, France; and ¶Department of Pathology, Fujita Health University School of Medicine, Aichi, 470-1192, Japan

A novel idea is emerging that a large molecular repertoire is common to the nervous and immune systems, which might reflect the existence of novel neuronal functions for immune molecules in the brain. Here, we show that the transmembrane adaptor signaling protein CD3ζ, first described in the immune system, has a previously uncharacterized role in regulating neuronal development. Biochemical and immunohistochemical analyses of the rat brain and cultured neurons showed that CD3ζ is mainly expressed in neurons. Distribution of CD3ζ in developing cultured hippocampal neurons, as determined by immunofluorescence, indicates that CD3ζ is preferentially associated with the somatodendritic compartment as soon as the dendrites initiate their differentiation. At this stage, CD3ζ was selectively concentrated at dendritic filopodia and growth cones, actin-rich structures involved in neurite growth and patterning. siRNA-mediated knockdown of CD3ζ in cultured neurons or overexpression of a loss-of-function CD3ζ mutant lacking the tyrosine phosphorylation sites in the immunoreceptor tyrosine-based activation motifs (ITAMs) increased dendritic arborization. Conversely, activation of endogenous CD3ζ by a CD3ζ antibody reduced the size of the dendritic arbor. Altogether, our findings reveal a novel role for CD3ζ in the nervous system, suggesting its contribution to dendrite development through ITAM-based mechanisms.

INTRODUCTION

Neuronal communication requires the formation of neuronal circuitry, achieved by a coordinated development of axons and dendrites. The ability of dendrites to receive and process neuronal signals is greatly determined by the dendritic architecture elaborated during development. It is now well established that dendrite formation is regulated by multiple factors that precisely control the extent of dendritic outgrowth and branching. Neuronal activity (Lohmann *et al.,* 2002), diffusible cues such as semaphorins and Slits (Polleux *et al.,* 2000; Whitford *et al.,* 2002), and intracellular signaling molecules (Fink *et al.,* 2003) have all been shown to regulate various steps of dendrite development. Interestingly, a large number of the aforementioned factors are also involved in the differentiation and function of other cell types in the immune system. For example, semaphorins and Slits are required for the maturation, migration, and activation of T lymphocytes and dendritic cells (Wu *et al.,* 2001; Kumanogoh and Kikutani, 2003). This common molecular repertoire

Abbreviations used: ITAM, immunoreceptor tyrosine-based activation motif; TCR, T-cell receptor; DIV, day in vitro.

shared by different biological systems emphasizes the existence of similar mechanisms underlying fundamental functions in cell differentiation, maturation and activation. Conversely, the expression and the role of several proteins thought to be specific for the immune system have recently been extended to the CNS (Boulanger and Shatz, 2004). This is the case for the CD3 subunit CD3ζ, a transmembrane adaptor signaling protein only characterized to date in T lymphocytes and natural killer (NK) cells, which associates to different cell surface receptors depending on the cell type (Lanier, 2001; Pitcher and van Oers, 2003). In T-cells, CD3ζ is a component of the CD3 complex, the signaling module of the T-cell receptor (TCR) that recognizes peptide fragments presented by major histocompatibility complex (MHC) molecules and is thus responsible for antigenic recognition (Samelson *et al.,* 1985). CD3ζ is instrumental in these processes because it is required for receptor-mediated signal transduction through its three copies of immunoreceptor tyrosine-based activation motif (ITAM; Pitcher and van Oers, 2003). Moreover, CD3ζ also participates in intrathymic T-cell differentiation, which is arrested in mice lacking CD3ζ (Malissen *et al.,* 1993). Brain analysis of these CD3ζ-deficient mice showed a striking abnormal development of the retinogeniculate projections in the visual system (Huh *et al.,* 2000). Defects in synaptic plasticity recorded in the hippocampus were also observed with an enhanced LTP and a lack of LTD (Huh *et al.,* 2000; Barco *et al.,* 2005). These findings suggest a novel role for CD3ζ in the development of the nervous system as well as in synaptic functions. How-

ever, the cerebral expression of CD3ζ proteins and the identity of CD3ζ-expressing cells have yet to be elucidated. In this study, we show that CD3ζ is predominantly expressed in neurons where it selectively localized at dendritic growth cones and filopodia. CD3ζ loss-of-function experiments in cultured neurons increased dendritic arborization, whereas activating endogenous CD3ζ inhibited dendritic branching. Altogether, our findings reveal a novel role for CD3ζ in the nervous system, highlighting its contribution to neuronal development.

MATERIALS AND METHODS

All protocols were carried out in accordance with French standard ethical guidelines for laboratory animals (Agreement 75-669).

Antibodies

Two commercially available anti-CD3ζ affinity-purified rabbit polyclonal antibodies were used for CD3ζ immunodetection. The first antibody (Ab36) was raised against aa 36–54, corresponding to an intracellular sequence of the protein (Spring Bioscience, Fremont, CA). The second antibody (Ab22) was raised against aa 22–30, a sequence corresponding to the N-terminus extracellular region of the protein (Alexis Bioscience, San Diego, CA). The mouse monoclonal antibodies to tau (antibody tau-1, clone PC1C6), microtubule-associated protein 2 (MAP2, clone AP20), neuronal nuclei (NeuN), and glyceraldehyde-3-phosphate dehydrogenase (GAPDH; clone 6C5) were purchased from Chemicon (Billerica, MA). The mouse monoclonal β-tubulin isotype III antibody (Tuj1, clone SDL.3D10) and the mouse monoclonal anti-glial fibrillary acidic protein (GFAP) were obtained from Sigma (St. Louis, MO) and the rabbit polyclonal tau from Dako (Glostrup, Denmark). The mouse monoclonal anti-oligodendrocyte (RIP) was purchased from Developmental Studies Hybridoma Bank (University of Iowa, Iowa City, IA) and anti-CD90 (clone OX7) was purchased from Bioatlantic (Nantes, France). The mouse anti-CD11b/c (clone OX42) and anti-CD161 (clone 3.2.3) were produced in our laboratory from hybridomas obtained from the European Collection of Animal Cell Culture (Salisbury, United Kingdom). The mouse mAb anti-CD45 receptor (CD45R, clone HIS24) was purchased from BD Biosciences (San Jose, CA). Peroxidase-conjugated goat anti-rabbit and biotinylated- and fluorescein isothiocyanate (FITC)-conjugated donkey anti-rabbit secondary antibodies were purchased from Jackson Laboratory (Bar Harbor, ME). The aminomethylcoumarin acetate (AMCA)-conjugated streptavidin was obtained from Beckman Coulter (Fullerton, CA) and the Alexa Fluor 568 goat anti-rabbit and goat anti-mouse were obtained from Invitrogen (Carlsbad, CA)

PCR Analysis

Total RNA was extracted from 50 to 100 mg of rat brain and spleen by homogenization in 1 ml of Trizol reagent (Invitrogen, Carlsbad, CA) for 5 min at room temperature followed by chloroform extraction and isopropanol precipitation. After centrifugation and washing in ethanol, RNA was resuspended in water and frozen at $-20°C$ until use. After Turbo DNAse treatment (Invitrogen), 2 μg of RNA were reverse-transcribed with a MMLV-reverse transcriptase system (Invitrogen). The synthesized cDNA was denatured for 2 min at 92°C, and 100 ng was subjected to 35 cycles of PCR amplification (92°C for 30s, 60°C for 30s, 72°C for 1 min, and a final extension step at 72°C for 5 min) in a total volume of 25 μl containing 0.4 μM of sense and antisense primers, 0.5 U of Taq polymerase (Invitrogen), and 200 μM of dNTP. For the amplification of CD3ζ mRNA, the sense oligonucleotide primer was 5'TC-GAGGAATTCCCACCATGAAGTGGACGGCATCAGTC-3' and the antisense oligonucleotide primer was 5'-TGACGACCGGTGCGCGAGGGGGC-AGGGTCTG-3', giving rise to a 152-base pair fragment. Internal standards were generated by amplifying the hypoxanthine-guanine phosphoribosyl-transferase (HPRT) mRNA using the following set of primers: sense, 5'-TTCCTCCTCAGACCGCTTTT-3' and antisense, 3'-CTTATAGCCCCCCT-TCAGCA-5', giving rise to a 262-base pair amplification product. PCR products were loaded on a 2% agarose gel.

Slice Preparation

Adult male Sprague-Dawley rats weighing 200 g were deeply anesthetized with Rompun-ketamine (1:4) at 1 ml/kg (i.p.). They were then perfused transcardially with 250 ml of 4% paraformaldehyde (PFA) in phosphate-buffered saline (PBS). Brains were dissected and postfixed in the same solution for 1 h at room temperature and then were cryoprotected overnight at 4°C in a solution of 15% sucrose in PBS and then 48 h at 4°C in 30% sucrose in PBS. Coronal sections (30 μm thick) were cut on a cryostat and collected in 0.1 M phosphate buffer (PB), pH 7.4.

Cell Cultures

COS-7 cells were grown in DMEM containing 10% fetal calf serum (FCS), 100 μg/ml streptomycin, and 100 U/ml penicillin.

Neural stem cell cultures were prepared from whole brains of E15 rat embryos as previously described (Sergent-Tanguy *et al.*, 2006). Briefly, tissues freed of meninges were incubated with 0.25% trypsin for 15 min at 37°C, and after addition of 10% FCS and 10 mg/ml DNAse I, were dissociated by mechanical trituration. Aggregates were removed by decantation and cells were further purified from small debris by centrifugation. The cell suspension was then incubated for 12 h in basal culture medium composed of DMEM containing Hams' F12 (1/1, vol/vol), 3 mM glucose, 5 mM HEPES (pH 7.2), 100 μg/ml streptomycin, and 100 U/ml penicillin (basal medium) and supplemented with 10% FCS (complete medium), and the uncoated cells were transferred to basal medium supplemented with N2 (Invitrogen) and 10 ng/ml FGF-2 to allow for the formation of neurospheres. After 5 d of culture, neurospheres were dissociated by trypsin and mechanical trituration to give a single-cell suspension. This was then plated on poly-L-ornithine–coated glass coverslips at a density of 3×10^4 cells/cm² for 2 h in complete medium and subsequently fixed in 4% PFA and 4% sucrose in PBS.

Glia cultures were prepared from newborn rat forebrains. Briefly, cortexes were dissected and dissociated by trypsin and DNAse and the cells were plated at a density of 35×10^3 cells/cm² in MEM containing 10% FCS, 0.6% D-glucose, 100 μg/ml streptomycin, and 100 U/ml penicillin. The medium was replaced with serum-free MEM containing N2 supplements 24 h before the neuron culture.

Rat hippocampal and cortical cultures were prepared from 18-d-old rat embryos by previously described methods (Goslin *et al.*, 1998; Pujol *et al.*, 2005). Briefly, hippocampi were dissected and dissociated by trypsin and trituration and plated on glass coverslips coated with poly-L-lysine. For calcium imaging assays and transfection, cells were plated at a density of 18×10^3 cells/cm². For all other uses, cells were plated at 4×10^3 cells/cm². The cells were allowed to attach on coverslips before being transferred to a dish containing a glial feeder layer, prepared as described above, and maintained for up to 21 d in serum-free MEM with N2 supplements. Neurons were used for immunocytochemical staining and morphology analysis 3 h after plating or after 1, 2, 4, 7, 10, and 21 d in vitro (DIV). For Western blot analysis, cells were collected at 7 DIV.

Western Blot Analysis

For Western blot analysis, homogenates from CD3ζ-transfected COS-7 cells, 7 DIV cultured neurons, T lymphocytes, and rat forebrain and spleen were prepared. Briefly, cultured neurons and COS-7 cells were scraped into PBS containing a cocktail of protease inhibitors and were then pelleted and resuspended in Laemmli buffer. T lymphocytes were isolated from total splenocytes after nylon wool adherence and depletion of CD161 (NK cells), CD11b/c (monocytes), and CD45R (B lymphocytes) positive cells using magnetic beads (Invitrogen/Dynal, Carlsbad, CA). For tissue preparation, rat forebrains and spleens were homogenized using a glass Teflon homogenizer in 10 mM Tris-HCl, pH 7.4, containing 320 mM sucrose and a cocktail of protease inhibitors. The resulting suspension was centrifuged at $700 \times g$ for 10 min. The supernatant was collected and centrifuged at $150,000 \times g$ for 30 min, and the pellet was resuspended in 10 mM Tris-HCl, pH 7.4. The membrane preparation was solubilized in Laemmli buffer.

Cell suspensions (~500,000 cells) and tissue homogenates (30 μg of protein) were loaded on an SDS-PAGE (12% acrylamide) and transferred to a nitrocellulose membrane. The membrane was blocked with 5% dried milk in 20 mM Tris-HCl, pH 7.4, containing 0.45 M NaCl and 0.1% Tween 20 (TBST). The membrane was then incubated overnight in Ab36 CD3ζ antibody (2.5 μg/ml) or with anti-GAPDH antibody (0,2 μg/ml), diluted in TBST containing 5% dehydrated milk, washed with TBST, incubated for 1 h in peroxidase-conjugated goat anti-rabbit antibody (1:3000) or in peroxidase-conjugated donkey anti-mouse antibody (1:2000), respectively, and visualized using a chemiluminescent substrate (Pierce, Rockford, IL) and exposure to x-ray films.

Immunostaining

For immunohistochemistry on rat brain sections, sections were first incubated in 0.3% H_2O_2 in 0.1 M PB for 30 min and, after two washes in PB, were additionally incubated for 30 min in 3% normal donkey serum (NDS) in PB. After two washes in PB, sections were incubated overnight at 4°C with Ab36 (0.2 μg/ml) or Ab22 (5 μg/ml) CD3ζ antibodies diluted in PB containing 3% NDS and 0.05% Triton X-100. The following day, sections were washed twice in PB and incubated for 45 min in biotinylated goat anti-rabbit IgG diluted at 1:200 in PB containing 0.5% NDS, followed by 45 min in streptavidin-biotine peroxidase solution (ABC Vectastain, Vector Laboratories, Burlingame, CA). After several rinses in PB, sections were further incubated in 0.05% 3,3'diaminobenzidine (Vector Laboratories) for 10 min at room temperature and were then mounted on gelatin-coated slides, dehydrated in graded ethanol, delipidated in xylene, cover-slipped with Eukit, and examined with a Zeiss microscope (Thornwood, NY). For control experiments, the primary antibodies were omitted during the procedure. For double immunofluorescence labeling, sections were incubated overnight at 4°C with Ab36 CD3ζ antibody and either anti-GFAP (1:500), anti-NeuN (1:200), anti-CD11b/c (1:500), or

anti-RIP (1:500) antibodies diluted in PB containing 3% NDS and 0.05% Triton X-100. Slices were then incubated for 1 h with the appropriate FITC- or Alexa Fluor 568–conjugated secondary antibodies (1:200 and 1:1000, respectively) and mounted with Vectashield (Vector Laboratories) on glass slides for analysis on an Axioskop 2 plus microscope (Zeiss). Pictures were acquired with 10× and 20× objectives using a digital camera (AxioCam HRC, Zeiss) driven by AxioVision Release 4.2 software. Two animals were analyzed to determine the phenotype of CD3ζ-expressing cells in the brain. For each animal, the number of CD3ζ-positive cells was recorded in the neocortex from two slices (300 CD3ζ-positive cells per slice), and the number of CD3ζ-positive cells that were also immunoreactive for GFAP (astrocyte), NeuN (neuron), CD11b/c (microglia), or RIP (oligodendrocytes) was counted. Images for presentation were prepared for printing with Adobe Photoshop (San Jose, CA). For neural stem cells and cultured neurons, cells were fixed in 4% PFA for 15 min, permeabilized for 5 min in 0.25% Triton X-100 in PBS, and incubated for 30 min in 10% bovine serum albumin (BSA) in PBS at 37°C. Cells were then incubated overnight in Ab36 CD3ζ antibody (2.5 μg/ml) or CD90 antibody (3 μg/ml) diluted in PBS containing 3% BSA. For double labeling, Ab36 CD3ζ antibody was mixed with either MAP2 (1:200), tau-1 (1:500), or Tuj1 (1:1000) antibodies. F-actin was labeled with TRITC-phalloidin (1:10000, Sigma Aldrich) for 1 h at 37°C before immunostaining. Cells were then incubated with the appropriate secondary antibodies conjugated to FITC, biotin (1:200), or Alexa Fluor 568 (1:1000). When the biotin-conjugated antibody was used, cells were subsequently incubated in AMCA-conjugated streptavidin (1:200). For double labeling on brain sections or cultured cells, control experiments achieved by omitting one of the primary antibodies showed the lack of cross-reactivity between the secondary antibodies and the absence of signal spillover between the two channels. The coverslips were mounted with Vectashield on glass slides for analysis on an Axioskop 2 plus microscope (Zeiss). Pictures were acquired with 20× and 63× objectives using a digital camera as described above.

DNA Constructs and Small Interfering RNA

A plasmid encoding rat CD3ζ fused at the C terminus with enhanced green fluorescent protein (EGFP) was produced. The coding sequence of CD3ζ containing a Kozak sequence at the 5′ end was obtained by PCR amplification and subcloned in frame into the EcoRI-AgeI sites of pEGFP-N1 to generate the CD3ζ-GFP expression plasmid.

To generate a mutant form of CD3ζ with the six tyrosine residues substituted by phenylalanine in the three ITAMs, 100 ng of the following three primers bearing the mutations—5′-AACCAGCTCTTTAACGAGCTCAAT-CTAGGGCGAAGAGAGGAATTTGATGTTTTG-3′, (5′-AAGGCGTGTTCA-ATGCACTGCAGAAAGACAAGATGGCAGAGGCCTTCAGTGAGATT-3′, and (5′-ACGGCCTTTTCCAGGGTCTCAGCACTGCCACCAAGGACACCT-TTGACGCCCTG-3′—were mixed with 100 ng of CD3ζ-GFP DNA template. The reaction was performed using the QuickChange Multi Site-Directed Mutagenesis Kit (Stratagene, La Jolla, CA) according to the manufacturer's instructions. All the CD3ζ cDNA constructs were confirmed by sequencing.

For small interfering RNA (siRNA) experiments, four sense and antisense oligonucleotides corresponding to the following cDNA sequences were purchased from Ambion (Austin, TX): 5′-GCAAAAUUCAGCAGGAGUGtt-3′ and 5′-CACUCCUGCUGAAUUUUGCtc-3′, siRNA1, nucleotides 276–294; 5′-GCUCUAUAACGAGCUCAAUtt-3′ and 5′-AUUGAGCUCGUUAUA-GAGCtg-3′; siRNA2, nucleotides 329–347; 5′-GGUAACAUGUAAUUAG-GUCtt-3′ and 5′-GACCUAAUUACAUGUUACCtt-3′, siRNA3, nucleotides 1066–1084; and 5′-GGCGUGUACAAUGCACUGCtt and 5′-GCAGUG-CAUUGUACACGCCtt; siRNA4, nucleotides 444–462). A control siRNA (Ambion), which showed no homology to any known gene sequences from rat, mouse, or human, was used as a negative control.

Transfections and Pharmacological Treatments

Transfection of COS-7 cells with the CD3ζ-expressing plasmid pRZ-3 (Itoh *et al., 1993*) was performed using the Lipofectamine 2000 reagent (Invitrogen) as previously described (Baudouin *et al.,* 2006). To determine which siRNA was the most effective in reducing CD3ζ protein expression, COS-7 cells were cotransfected with 3 μg of pRZ-3 and 50 nM of either siRNA1, 2, 3, or 4 or negative control using the Lipofectamine 2000 reagent. One day after transfection, cells were collected to analyze CD3ζ protein expression by Western blot.

Neuron transfection was performed at 3 DIV with 3 μg of either CD3ζ-GFP cDNA or 3 μg of CD3ζ-6Y6F-GFP or 3 μg of membrane-targeted GFP (mGFP) cDNA [GAP-GFP(S65T), a gift from Dr. K. Moriyoshi, Kyoto University, Japan; Moriyoshi *et al.,* 1996], using 3 μl of the Lipofectamine 2000 reagent. The cells were fixed in 4% PFA and 4% sucrose in PBS at 5 DIV for MAP2 and tau double labeling.

For siRNA assays, neurons were cotransfected at 3 DIV with 3 μg of mGFP cDNA and 50 nM of siRNA1 or siRNA3 using 3 μl of the Lipofectamine 2000 reagent. The cells were fixed in 4% PFA and 4% sucrose in PBS at 5 DIV for MAP2 and CD3ζ double immunolabeling.

For antibody treatments, either 5 μg/ml Ab22 CD3ζ antibody or 5 μg/ml control antibody to human CD16 (3g8) were added to neuron cultures at 1 and 3 DIV. In control cultures the same volume of vehicle was added. Cells

were fixed in 4% PFA and 4% sucrose in PBS at 5 DIV and were immunolabeled for MAP2 morphological analysis.

To assess the effects of inhibiting protein kinases on CD3ζ distribution, neurons were treated at 7 DIV for 5, 15, 30, 60, and 120 min with 10 μM piceatannol (Sigma) an inhibitor of the Syk/ZAP70 family of the protein tyrosine kinases, 100 nM damnacanthal (Calbiochem, San Diego, CA) a specific inhibitor of lck, a protein tyrosine kinase of the Src family, 1 μM PP2 (Sigma), a broad inhibitor of the Src-family protein tyrosine kinases (Sigma), or 50 nM wortmannin (Sigma), an inhibitor of phosphoinositide 3-kinase. All the kinases inhibitors were added directly to the culture medium from a concentrated DMSO stock. To test the role of the actin cytoskeleton on CD3ζ localization, neurons were treated for 30 min and 3 and 24 h with 1 μM cytochalasin D (Sigma) added to the culture medium from a concentrated DMSO stock.

Quantification of CD3ζ Expression and Neuronal Morphology Analysis

To quantify CD3ζ or GAPDH expression in CD3ζ-expressing COS-7 cells after siRNA transfection, the signal intensity obtained on Western blot membranes was measured from four experiments using Image J software (http://rsb.in-fo.nih.gov/ij/) and expressed as a percentage of the intensity obtained from control cells without siRNA. To quantify CD3ζ immunoreactivity in neurons after siRNA transfections, coverslips were scanned on the microscope with a 10× lens and pictures of transfected cell were acquired with a 40× objective. The intensity of CD3ζ immunofluorescence was measured with the Image J software in well-isolated GFP-positive neurons cotransfected with either control or CD3ζ siRNAs and in nontransfected neurons located nearby the transfected cells. The intensity of CD3ζ immunoreactivity was measured in the dendritic field, but excluding the cell body, because CD3ζ was mainly targeted to dendrites and because the thickness of the cell body is a frequent source of nonspecific labeling compared with the nerve processes. A total of 16–34 cells per experimental condition were analyzed from two independent experiments. For each individual experiment, 3–7 cells were scored from at least two coverslips. Results are presented as average ± SEM of the ratio of anti-CD3ζ fluorescence intensity in GFP-positive neurons relative to nearby nontransfected neurons.

To analyze the morphology of neurons transfected with control siRNA, siRNA1, siRNA3, mGFP, CD3ζ-GFP, or CD3ζ-6Y6F-GFP, each coverslip was systematically scanned with a 10× lens and acquired with a 40× or 63× objective. Images from mGFP-labeled neurons were projected on the computer screen, all primary dendritic branches were traced with the mouse using the ImageJ software program, and the number and length of dendritic branches were scored. As defined in previous studies using a model of hippocampal neuron culture, protrusions with a length <10 μm likely corresponded to filopodia and dendritic spines, whereas protrusions with a length >10 μm were defined as dendritic branches (Jaworski *et al.,* 2005; Terry-Lorenzo *et al.,* 2005). Consequently, only the protrusions with a length >10 μm were taken into account to quantify the number and length of dendritic branches. Between 10 and 15 cells were scored from at least two coverslips for each experimental condition. A total of 29–63 cells were analyzed for each experimental condition from two to four independent experiments, and the data were presented as average ± SEM. To analyze experiments involving neuron cultures treated with either 3g8 or CD3ζ antibody, images from MAP2-labeled neurons were randomly acquired with a 20× and 40× lens, and the number and length of dendritic branches was measured as above. Data are presented as average ± SEM of a total of 40–52 cells per experimental condition recorded from two to four coverslips (5–10 cells per coverslips) obtained from two to three independent neuron cultures. Data analysis was performed using Excel (Microsoft, Redmond, WA) and GraphPad Prism 4 (San Diego, CA), and statistical analyses were done by Student's *t* test. Images were processed and prepared for printing using Adobe Photoshop.

Fluorescence Measurements of Intracellular Calcium

The effects of Ab22 CD3ζ antibody on intracellular calcium concentration ([Ca^{2+}]$_i$) in 7 DIV cultured neurons were assessed using the calcium-sensitive fluorescent probe Fluo-3 AM (Molecular Probes). Neurons were loaded with 4 μM Fluo-3 AM in Tyrode (145 mM NaCl, 4 mM KCl, 1 mM MgCl$_2$, 1 mM CaCl$_2$, 5 mM HEPES, and 5 mM glucose) and 0.02% Pluronic at 37°C for 30 min. The coverslips were mounted on the stage of an inverted microscope (Nikon Diaphot, Tokyo, Japan) equipped for fluorescence and illuminated at 450–490 nm. The emitted light (>515 nm) was collected by a high-resolution image intensifier coupled to a video camera (Extended ISIS camera system; Photonic Science, Roberts-bridge, United Kingdom) and connected to a digital image processing board controlled by FLUO software (Imstar, Paris, France). Cells were maintained at 37°C and continuously superfused with Ca^{2+}-free Tyrode. A microperfusion system allowed for local application and rapid change of the different experimental media. Microperfusion solutions were identical to the Ca^{2+}-free Tyrode except that they contained 20 mM mannitol for efficient local perfusion of the neurons under analysis. Single-cell fluorescence intensity was measured from digital image processing and displayed against time. Fluorescence intensity was normalized to the intensity measured
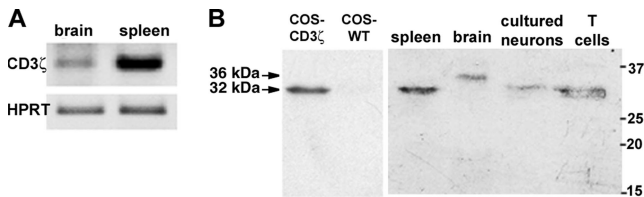
Figure 1. Expression of CD3ζ in the rat brain and in cultured neurons. (A) Expression of CD3ζ mRNA in the rat brain. PCR amplification of CD3ζ mRNA extracted from adult rat brain and spleen (positive control). HPRT amplification products indicated that PCR was performed on comparable levels of RNA. (B) Identification of heterologously expressed and endogenous CD3ζ by Western blot. Cell homogenates of nontransfected (COS-WT) and CD3ζ-transfected (COS-CD3ζ) COS-7 cells, as well as membrane homogenates prepared from rat spleen, brain, 7 DIV cultured neurons, and T-cells were resolved on a 12% SDS-PAGE and immunoblotted with Ab36 CD3ζ antibody. An immunoreactive band can be observed at 32 kDa in CD3ζ-transfected COS-7 cells, spleen, cultured neurons, and T-cells and at 36 kDa in brain homogenates. Molecular weight markers are indicated on the right.

before antibody application. Calcium variations were quantified by a linear regression of the first 10 points of the fluorescence curve after antibody application ($\Delta F/F/t$ in s^{-1}).

RESULTS

Expression of CD3ζ in the Rat Brain and in Cultured Neurons

To examine whether CD3ζ mRNA was expressed in the brain, RT-PCR amplifications of CD3ζ was performed on total RNA extracted from rat forebrain and compared with the spleen. Amplification of HPRT transcripts served as an internal control to confirm RNA integrity for each preparation. In brain samples, a band of the expected size of 152 base pairs was detected, although exhibiting a lower intensity than in spleen preparations (Figure 1A). The expression of CD3ζ at the protein level was investigated by Western blot experiments under nonreducing conditions to preserve the disulfide bridge of the homodimer forms of CD3ζ known to be prevalent in immune cells (Baniyash, 2004). Western blots of COS-7 cells transfected with rat CD3ζ cDNA showed that the Ab36 CD3ζ antibody yielded a single band of 32 kDa, whereas no signal was apparent in nontransfected cells (Figure 1B). In the spleen, T-cells and cultured neurons, the 32-kDa form was also detected, whereas a 36-kDa band was present in rat brain homogenates (Figure 1B), a molecular weight in agreement with the 37-kDa form of CD3ζ reported in hippocampus preparations (Sourial-Bassillious *et al.*, 2006). The characterization of the molecular forms of CD3ζ expressed in heterologous COS-7 cell systems, splenocytes, and peripheral T-cells have been well established, which showed that the nonphosphorylated CD3ζ homodimer exhibited an apparent molecular weight of 32 kDa and that activation-induced tyrosine phosphorylation of the ITAMs resulted in the appearance of multiple forms with molecular weights ranging from 36 to 45 kDa depending on the number of phosphorylated tyrosine residues (Sancho *et al.*, 1993; Furukawa *et al.*, 1994; Garcia and Miller, 1997; van Oers *et al.*, 2000). Although the 32-kDa form of CD3ζ detected in CD3ζ-transfected COS-7 cells, spleen, T-cells, and cultured neurons likely corresponds to a nonphosphorylated CD3ζ homodimer, the 36-kDa band detected in the brain might reflect the existence of a constitutively phosphorylated form of CD3ζ in cerebral tissue.

We next examined the expression pattern of CD3ζ protein in rat brain slices by immunohistochemistry with the anti-CD3ζ antibodies Ab36 and Ab22. Using both antibodies, CD3ζ immunoreactivity was widely distributed in numerous brain areas, including the cerebral cortex and hippocampus (Figure 2, A–F). Importantly, the distribution of CD3ζ immunoreactivity displayed by Ab36 strongly paralleled that obtained with Ab22, both at regional and cellular levels, supporting the specificity of the immunolabeling produced by both antibodies (compare Figure 2, B–E, with Figure 2, B′–E′). CD3ζ immunolabeling was extensively associated with neurons, as assessed by double labeling with the neuronal marker NeuN (Figure 2G) and was shown to outline the periphery of cell bodies and to be associated with dendritic processes (Figure 2, C, C′, and F). The phenotype of CD3ζ-expressing cells in brain slices was further analyzed in the neocortex by counting the number of CD3ζ-positive cells that were also immunoreactive for NeuN (neuron), RIP (oligodendrocyte), or GFAP (astrocyte), or CD11b/c (microglia). The quantification indicated that 91 ± 2 and $4 \pm 1\%$ of the total CD3ζ-expressing cells (n = 1200 from two rats) were associated with neurons or oligodendrocytes, respectively (Figure 2, G and H). The remaining was associated with unidentified profiles. Conversely, $88 \pm 5\%$ of neurons (n = 1300) and $44 \pm 6\%$ of oligodendrocytes (n = 117) were immunopositive for CD3ζ. No labeling was observed within astrocytes and microglia (Figure 2, I and J). Altogether, the biochemical and immunostaining data obtained with the Ab36 and Ab22 antibodies are consistent with a prominent constitutive neuronal expression of CD3ζ in the brain and in cultured neurons.

CD3ζ Is Selectively Enriched at Growth Cones and Filopodia during Neuronal Development

All of the following immunostaining experiments were performed with Ab36 CD3ζ antibody. To determine at which stage of neuronal development CD3ζ started to be expressed, we first used primary cultures of neural precursor cells grown as neurospheres, a free-floating cellular aggregate formed of neural stem cells (Reynolds *et al.*, 1992). After dissociation of the neurospheres into a single cell suspension and plating onto glass coverslips, neural stem cells initiated their differentiation to generate neuronal and glial cells. This culture system allowed to obtain neuroblasts at a very immature stage, only a few hours after the initiation of their differentiation from neural stem cells. Two hours after plating, cells were double-labeled with Ab36 CD3ζ antibody and a tubulin β III (Tuj1) antibody used as a neuronal marker (Figure 3A). At this stage, $12 \pm 1\%$ of total cells (n = 346 cells) were immunopositive for Tuj1, and $72.5 \pm 6.4\%$ of Tuj1-positive cells (n = 43) were also immunolabeled for CD3ζ. Conversely, all of the CD3ζ-immunopositive cells were additionally immunopositive for Tuj1, indicating that CD3ζ was specifically expressed in newly differentiated neurons. Within these cells, CD3ζ immunoreactivity was mostly associated with the periphery of the cell, suggestive of a plasma membrane localization (Figure 3A).

To study the developmental pattern of CD3ζ distribution in neurons, we chose a low-density hippocampal neuron culture model for which the critical developmental stages have been well characterized (Dotti *et al.*, 1988). At 1 DIV, a stage corresponding to the emergence of few minor neurites and preceding the axonal polarization (stage 2; Dotti *et al.*, 1988), CD3ζ immunoreactivity was highly concentrated at the tip of growing neurites, closely associated with growth cones (Figure 3B). We found that $92 \pm 3\%$ of the neurites exhibited CD3ζ immunoreactivity at their tips (74 neurites
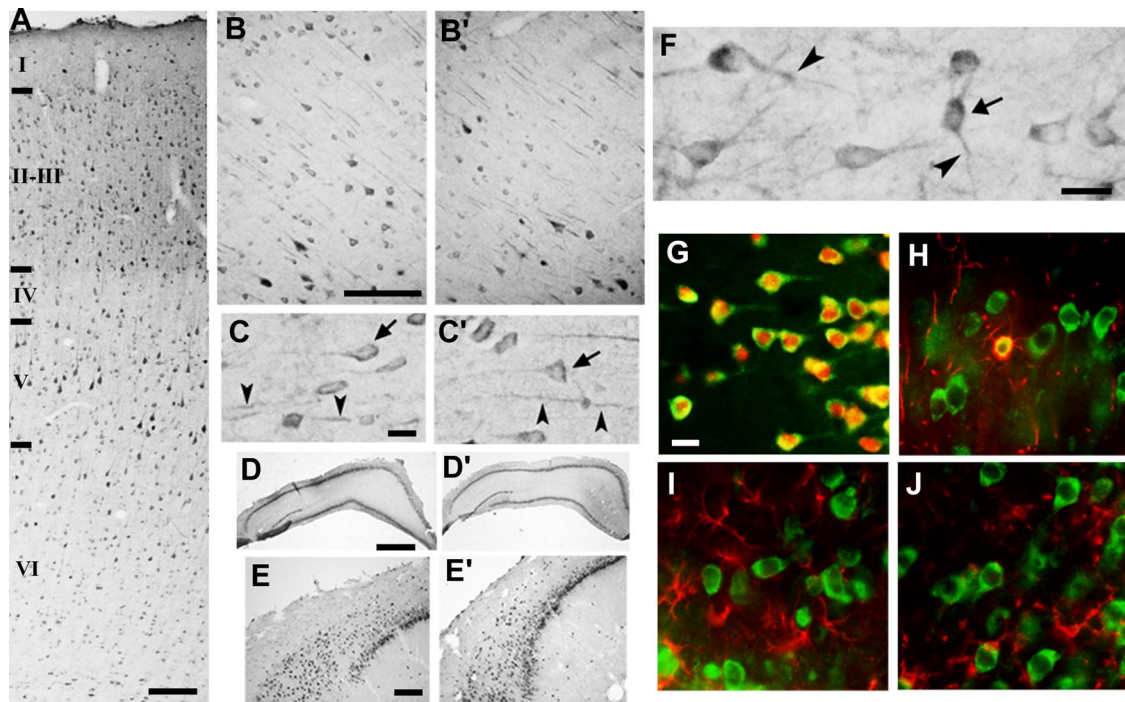
Figure 2. Distribution of CD3ζ immunoreactivity in the rat brain. (A) In the parietal cortex, CD3ζ-immunoreactive cells are detected throughout the six layers, but immunolabeled neuronal processes predominate in layers V and VI. (B–E') The comparison between the distribution of CD3ζ immunoreactivity in rat brain slices as revealed by Ab36 (B–E) and Ab22 (B'–E') antibodies. Both antibodies give rise to a virtually identical labeling pattern, as shown here in the cerebral cortex (B, B', C, and C') and hippocampus (D, D', E, and E'). At high magnification in the cerebral cortex (C and C') and in the dentate gyrus of the hippocampus immunolabeled with Ab36 (F), most CD3ζ-expressing cells exhibit a neuronal morphology and are immunolabeled within both perikarya (arrows in C, C', and F) and dendritic processes (arrowheads in C, C', and F). (G–J) Double immunolabeling of hippocampal sections with Ab36 CD3ζ antibody (green) and the markers (red) NeuN for neurons (G), RIP for oligodendrocytes (H), GFAP for astrocytes (I), and CD11b/c for microglia (J). Scale bars, (A) 300 μm; (B and E) 75 μm; (C, F, and G–J) 15 μm; (D) 1 mm.

analyzed from 18 cells). At 2 DIV, a stage of selective axon elongation in which the longest neurite corresponds to the growing axon (stage 3; Dotti *et al.,* 1988), CD3ζ was still accumulated at the tip of the processes, with equal distribution observed for axons and minor neurites (Figure 3C). In addition, high CD3ζ immunoreactivity was also detected within small nascent protrusions localized along neurites, corresponding to potential future ramifications (Figure 3C). At 4–5 DIV, characterized by continuing axonal growth and differentiation of minor neurites into dendrites (stage 4; Dotti *et al.,* 1988), CD3ζ distribution was similar to that observed at 2 DIV, with a further specific enrichment of CD3ζ immunoreactivity at the tips of processes. Nevertheless, unlike at 2 DIV, at 4–5 DIV CD3ζ showed a marked preferential localization with dendrites than with axons (Figure 3D), as confirmed by double-labeling experiments of CD3ζ with the dendritic marker MAP2 and the axonal marker tau-1 (Figure 4, A and B). Although CD3ζ immunoreactivity was observed in the somatodendritic domain of virtually all neurons, only a few immunopositive axons were detected. By 7–10 DIV (stage 5; Dotti *et al.,* 1988), which is marked by continued maturation of axonal and dendritic arbors, CD3ζ immunoreactivity was still highly compartmentalized at the tips of dendrites, and profusely associated with filopodia and spine-like protrusions of the somatodendritic domain (Figure 3, E and E'). At 21 DIV, when neurons have reached a mature stage characterized by the formation of synaptic contacts, CD3ζ immunoreactivity was distributed in clusters that largely overlapped with the postsynaptic marker PSD-95 (Figure 3, F and F'). However, not all, but

a subset of PSD95-expressing synapses was immunopositive for CD3ζ, and conversely a fraction of CD3z clusters were colocalized with PSD-95 (Figure 3F'). To examine in detail the CD3ζ cellular distribution within growth cones in young neurons, double-staining experiments on 3 DIV neurons were performed with Ab36 CD3ζ antibody and either TRITC-phalloidin or anti-tubulin β III antibody, to visualize the respective F-actin– and microtubule-rich regions of the growth cone (Figure 4, C and D). CD3ζ immunoreactivity largely overlapped with the actin meshwork concentrated in the peripheral region of the growth cone, but was only rarely associated with the extending filopodia (Figure 4C). The central region, characterized by bundles of microtubules was mostly devoid of CD3ζ labeling (Figure 4D). Altogether, analysis of the developmental pattern of CD3ζ immunoreactivity in cultured neurons showed that it is expressed early during neuron differentiation and is associated with growth cones and filopodial protrusions throughout development. As the neurons mature, CD3ζ immunoreactivity becomes mainly restricted to the somatodendritic compartment where it is enriched at synaptic sites.

CD3ζ Clustering at the Tips of Neurites Is Dependent on Filamentous Actin and Protein Tyrosine Kinases of the Syk/ZAP-70 Family

Because CD3ζ was associated with F-actin–rich regions, we tested the role of actin filaments in localizing CD3ζ at growth cones and filopodia. Neurons were treated with 1 μM cytochalasin D for 24 h to disrupt actin microfilaments and were subsequently immunostained for CD3ζ. This ma-
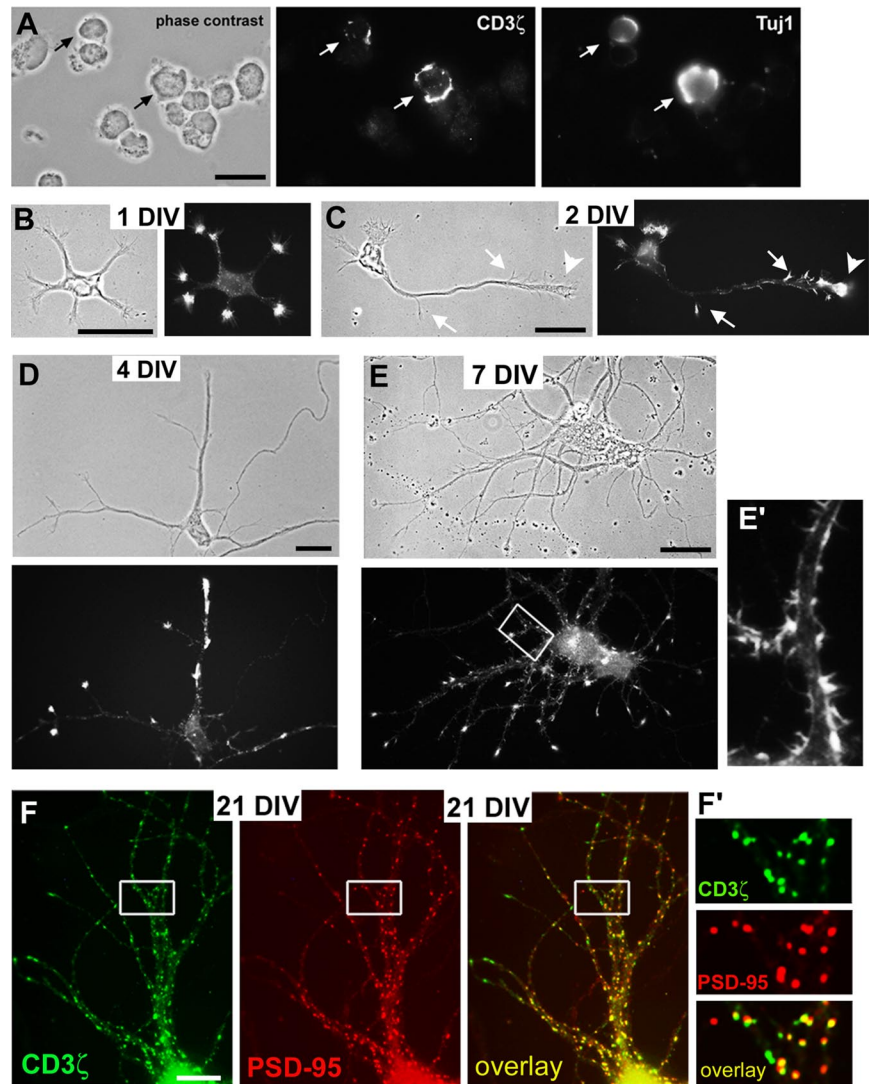
Figure 3. Developmental distribution of CD3ζ in neurons derived from neural stem cells and in hippocampal neurons in culture from 1 to 21 DIV. (A) Neural stem cells cultured as neurospheres were dissociated, plated on glass coverslips, and fixed 2 h later in PFA for the immunodetection of CD3ζ and Tuj1 (Tubulin β III), used as a neuronal marker. The immunopositive CD3ζ cells are all immunoreactive for Tuj1 (arrows), corresponding to newly differentiated neurons. (B–E) Hippocampal neuron cultures were fixed at 1 (B), 2 (C), 4 (D), 7 (E), and 21 (F) DIV and were immunolabeled for CD3ζ. From 1–7 DIV, the paired phase-contrast image is shown to visualize cell morphology. At 1 and 2 DIV (B and C), CD3ζ immunoreactivity is selectively associated with minor neurite endings, axonal growth cones (arrowhead in C), and protrusions emerging along the growing axon (arrows in C). At 4 DIV (D), CD3ζ immunoreactivity is highly enriched at the tips of dendrites and short branches. At 7 DIV (E) CD3ζ immunoreactivity is still observed at the tip of dendrites and branches and is also abundantly associated with filopodia and spine-like protrusions distributed along dendritic processes, as shown at higher magnification of the boxed region (E'). (F) Neurons at 21 DIV were fixed and immunolabeled for CD3ζ (green) and the postsynaptic marker PSD-95 (red). Numerous CD3ζ clusters are distributed along dendritic processes that partially colocalized with PSD-95 at synaptic sites as shown at higher magnification of the boxed region (F'). Scale bars, (A and B) 5 μm; (C) 10 μm; (D–F) 15 μm.

nipulation caused a pronounced redistribution of CD3ζ in numerous small puncta dispersed along dendrites but no longer concentrated at dendritic tips or filopodia (Figure 5A). Interestingly, the dispersed CD3ζ clusters remained highly associated with the translocated F-actin puncta, suggesting a close molecular interaction between CD3ζ and actin filaments (Figure 5B). Cytochalasin D treatment did not affect the distribution of Thy-1 (other name CD90), a GPI-linked membrane protein expressed on neurons in the nervous system (Morris, 1985; Mahanthappa and Patterson, 1992), suggesting that cytochalasin D did not cause a general remodeling of the neuronal plasma membrane that would affect the distribution of all membrane-associated proteins (Figure 5B). The cytochalasin D–induced redistribution of CD3ζ was significantly reversed after 3 h of cytochalasin D washout (Figure 5A), supporting a major role of actin in the dynamic regulation of CD3ζ clustering in and out of neurite endings and filopodia.

In immune cells, protein tyrosine kinases of the Syk/ZAP-70 family play a crucial role in the function of CD3ζ by regulating its association with effector molecules (Chan *et al.*, 1994). Considering the close relationships between the phosphorylation-regulated activation of signaling molecules and their subcellular distribution, we investigated whether inhi-

bition of Syk/ZAP-70 kinases would affect CD3ζ accumulation at growth cones and filopodia. Neurons at 7 DIV were treated from 5 min to 2 h with 10 μM piceatannol to inhibit Syk/ZAP-70, and CD3ζ distribution was studied by immunofluorescence. As of 5 min of piceatannol treatment, the CD3ζ immunoreactive clusters were completely dispersed, and a decrease in the overall staining intensity of CD3ζ was observed (Figure 5C). The piceatannol-induced CD3ζ dispersal was significantly reversible after 4 h of washout. Although the main action attributed to piceatannol is to inhibit Syk/ZAP-70 kinases, a few studies have reported that piceatannol might also inhibit the Src protein tyrosine kinase lck (Geahlen and McLaughlin, 1989). We thus tested whether a global inhibition the Src protein tyrosine kinases family (including lck) with 1 μM PP2 (Figure 5C) or a selective inhibition of lck with 100 nM damnacanthal, would affect CD3ζ distribution similarly as piceatannol. As another control, neurons were also treated with the phosphoinositide 3-kinase inhibitor wortmannin (50 nM). No modification of CD3ζ distribution was noticed upon PP2, damnacanthal, or wortmannin treatments compared with untreated neurons at any of the time points examined (from 5 min to 2 h). These data suggest that phosphorylation events medi-
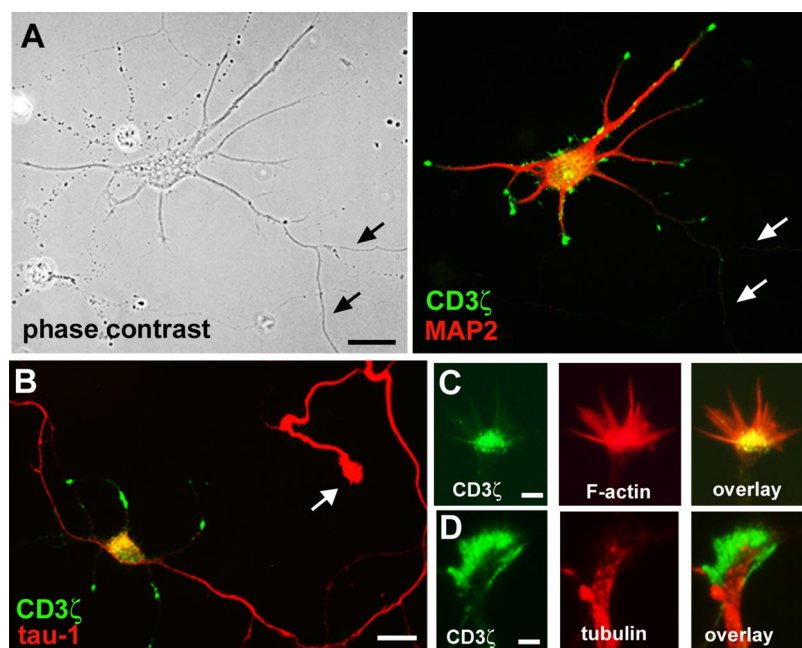
Figure 4. CD3ζ is concentrated at dendritic tips and filopodia and is selectively associated with the peripheral region of the growth cone. (A) Neurons at 7 DIV were fixed and immunolabeled for CD3ζ (green) and the dendritic marker MAP2 (red). CD3ζ-immunoreactivity is mostly confined to the somato-dendritic compartment and is not detected in the axon, defined as a MAP2-negative process (arrows). (B) Double labeling of CD3ζ (green) and the axonal marker tau-1 (red) of 7 DIV neurons show that the axonal trunk and growth cone (arrow) are devoid of CD3ζ immunoreactivity. (C) At growth cones of 2–3 DIV neurons, CD3ζ immunoreactivity (green) is localized to the peripheral actin-rich region labeled with TRITC-phalloidin (red), but is mostly excluded from the extending filopodia. (D) The central region of the growth cone, defined as a microtubule-rich region immunolabeled with Tuj1 antibody (red), is devoid of CD3ζ immunoreactivity. Scale bars, (A and B) 20 μm; (C and D) 2.5 μm.
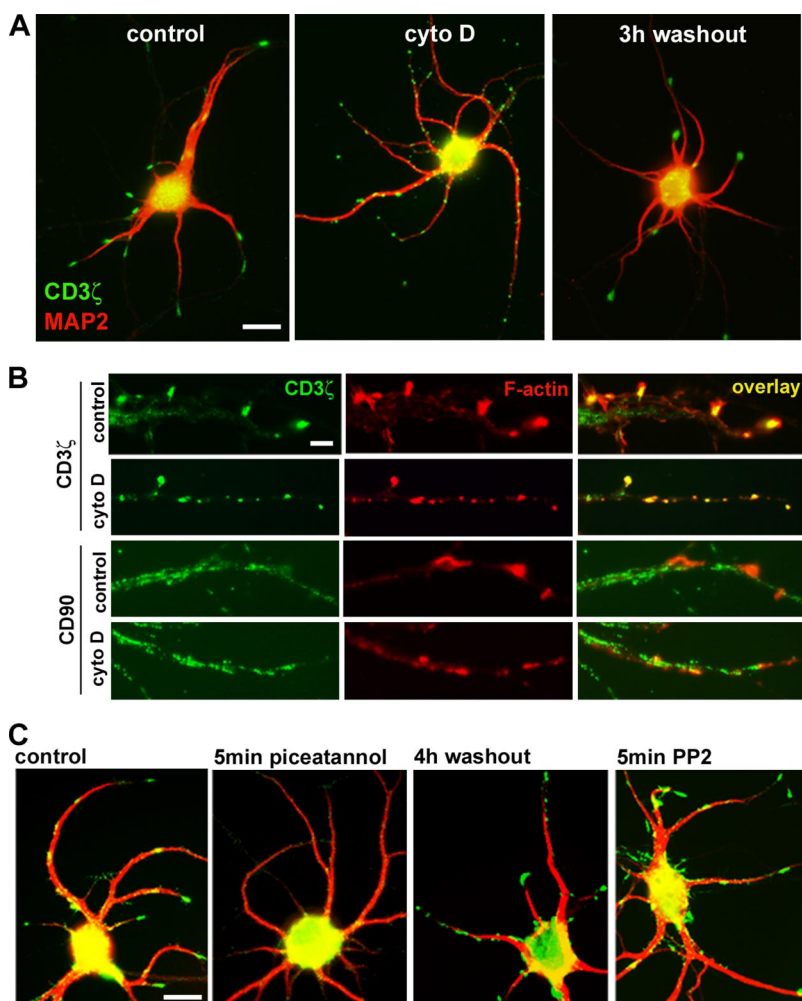

Figure 5. The selective concentration of CD3ζ at dendritic tips depends on filamentous actin and on protein tyrosine kinases of the Syk/ZAP-70 family. (A) Neurons at 7 DIV were either left untreated (control) or were exposed for 24 h to 1 μM of cytochalasin D to depolymerize actin (cyto D), and fixed and immunolabeled for CD3ζ (green) and MAP2 (red). Cytochalasin D treatment induced a redistribution of the large CD3ζ clusters localized at dendritic tips to small puncta dispersed along dendrites, whereas MAP2 immunostaining was unaffected. A 3-h washout after cytochalasin D treatment resulted in significant reversal that shows reaccumulation of CD3ζ at dendritic tips (3-h washout). (B) Control neurons and cytochalasin D–treated neurons are double-labeled for either CD3ζ or CD90 (green) and for F-actin with TRITC-phalloidin (red). In control neurons CD3ζ strictly colocalizes to F-actin–rich subdomains identified as filopodia and dendritic tips. In cytochalasin-treated neurons, CD3ζ remains associated to the dispersed F-actin puncta, which become evenly distributed within dendrites. The distribution of CD90 shows no relationship with F-actin labeling in control neurons and is unaffected by the cytochalasin D treatment. (C) Neurons at 7 DIV were either left untreated (control) or treated for 5 min with 10 μM piceatannol, an inhibitor of the protein tyrosine kinases of the Syk/ZAP-70 family, and were then immunolabeled for CD3ζ (green) and MAP2 (red). Blockade of the Syk/ZAP-70 kinases induces a rapid loss of CD3ζ aggregates, an effect reversed after 4 h of washout. By contrast, CD3ζ distribution was unaffected by 1 μM PP2, an inhibitor of the Src-family of protein tyrosine kinases. Scale bars, (A and C) 20 μm; (B) 2 μm.

ated by protein tyrosine kinases of the Syk/ZAP-70 family play a major role in regulating CD3ζ distribution in neurons.

CD3ζ siRNA and a CD3ζ Mutant Lacking the Sites of Tyr Phosphorylation Impairs Dendrite Formation

On the basis of our finding that CD3ζ proteins are specifically enriched at dendritic tips and protrusions during the stage of dendrite elaboration and maturation, we examined whether CD3ζ might play a role in dendrite development. For this purpose, we used an siRNA approach to knockdown CD3ζ protein expression in cortical neurons culture. Four CD3ζ siRNA sequences against different regions of CD3ζ were tested for their efficacy and specificity in suppressing CD3ζ expression in CD3ζ-transfected COS-7 cells (Figure 6A). We found by immunoblot analysis that two of them, siRNA1 and siRNA3, caused a marked reduction of the CD3ζ protein expression reaching 30.7 ± 6.1 and $7.5 \pm 5.2\%$, respectively, of the signal intensity of CD3ζ-expressing cells transfected with a control siRNA (Figure 6A). To test whether these siRNAs can decrease the expression level of endogenous CD3ζ in neurons, cultured neurons at 3 DIV were cotransfected with either siRNA1 or siRNA3 and mGFP as a marker of transfection, and CD3ζ immunoreactivity was quantified in the dendritic arbor at 5 DIV. The addition of siRNA1 or siRNA3 induced a severe reduction of endogenous CD3ζ level that dropped to $21.7 \pm 6.0\%$ (n = 23) and $14.5 \pm 5.1\%$ (n = 16), respectively, of the averaged CD3ζ signal intensity measured in nearby untransfected neurons (Figure 6, B and C). The control siRNA did not affect CD3ζ immunostaining as compared with neighboring untransfected cells ($98.7 \pm 14.8\%$, n = 34; Figure 6, B and C). The siRNA transfections were performed at 3 DIV, and the cells were analyzed at 5 DIV, a period corresponding to a stage of dendrite differentiation in this neuronal culture model (Dotti *et al.*, 1988). Therefore, these experiments allowed us to test the contribution of CD3ζ to dendrite formation. We observed that CD3ζ siRNA1 and siRNA3 significantly increased the size and the complexity of the dendritic arbor analyzed after immunostaining for CD3ζ and the dendritic marker MAP2. The total length of dendritic branches recorded per cell was increased by 90 and 123% upon transfection with siRNA1 or siRNA3, respectively, compared with control cells transfected with a control siRNA (control siRNA, 86.5 ± 11.1 μm, n = 63 cells; CD3ζ siRNA1, 163.3 ± 16.3 μm, n = 52 cells, p < 0.001; CD3ζ siRNA3, 192.6 ± 31.6 μm, n = 29 cells, p < 0.01, Student's *t* test; Figure 6, C–E). Moreover, the amount of dendritic branching recorded per cell was increased by 80 and 99% after transfection with CD3ζ siRNA1 or siRNA3, respectively, compared with siRNA control cells (control siRNA, 2.94 ± 0.34, n = 63 cells; CD3ζ siRNA1, 5.29 ± 0.45, n = 52 cells, p < 0.001; CD3ζ siRNA3, 5.86 ± 0.89, n = 29 cells, p < 0.01; Figure 6, C–E). There was no detectable difference in the dendritic arbor between either siRNA1 and siRNA3 (p = 0.43 for the branching length and p = 0.57 for the dendritic branchpoint number) or between mGFP and control siRNA (p = 0.63 for the branching length and p = 0.60 for the dendritic branchpoint number; values for mGFP are 79.1 ± 10.5 μm for the branching length, n = 56 cells, and 2.70 ± 0.31 for the number of dendritic branches, n = 56 cells), supporting that the changes in dendritic morphology induced by CD3ζ-targeted siRNAs were specifically linked to the reduced CD3ζ expression.

To further test the role of CD3ζ in dendrite outgrowth, we generated a putative dominant negative form of CD3ζ. In T lymphocytes, CD3ζ is the critical signaling subunit of the TCR-CD3 complex involved in the recognition of MHC-peptide complex present on antigen-presenting cells. The function of CD3ζ critically depends on its 3 ITAMs, a se-

quence motif containing two Tyr phosphorylation sites (YxxLx(6–8)YxxL). On TCR-MHC binding, Src family protein tyrosine kinases Lck or Fyn phosphorylates the Tyr residues in the ITAMs, triggering the T-cell response. Substitution of the six Tyr into Phe residues completely abolished the ability of CD3ζ to be phosphorylated and therefore converts CD3ζ into an inactive form (Lowin-Kropf *et al.*, 1998; van Oers *et al.*, 2000). We thus replaced the six Tyr of CD3ζ fused to GFP (CD3ζ-GFP) by Phe and the resulting CD3ζ-6Y6F-GFP construct was overexpressed in cultured neurons by transfection at 3 DIV. Neurons were transfected with mGFP alone as control. Cells were fixed at 5 DIV and immunostained for MAP2 to label dendrites. In neurons overexpressing the CD3ζ-6Y6F-GFP mutant, the dendrites were more elaborate than in the mGFP-transfected cells (Figure 7). Quantification revealed that the total branch length recorded per cell and branchpoint number per cell increased by 65 and 42%, respectively (for total branch length per cell, mGFP, 79.1 ± 10.5 μm, n = 56 cells; CD3ζ-6Y6F-GFP, 130.9 ± 18.8 μm, n = 32 cells, p < 0.01; for number of branchpoint per cell, mGFP, 2.70 ± 0.31, n = 56 cells; CD3ζ-6Y6F-GFP, 3.84 ± 0.46, n = 32 cells, p < 0.05; Figure 7). Thus, expression of CD3ζ-6Y6F-GFP affected dendritic development by promoting branchpoint formation, suggesting that CD3ζ may be normally involved in dendrite patterning, likely through an ITAM-based mechanism. Conversely, transfection with CD3ζ-GFP induced a reduction in the length and number of dendritic branches recorded per cell by 34% (52.5 ± 6.8 μm, n = 58 cells, p < 0.05) and 27% (1.97 ± 0.20, n = 58 cells, p = 0.051), respectively, compared with control cells transfected with mGFP (see values above; Figure 7). This result suggests that endogenous CD3ζ activity was limiting in dendrite patterning and that increasing CD3ζ concentration through neuron transfection with CD3ζ-GFP further inhibited dendrite development. Altogether, these results suggest that neuronal CD3ζ is a negative regulator of dendrite outgrowth and patterning.

Application of CD3ζ Antibody to Cultured Neurons Elicits Intracellular Calcium Increase and Inhibits Dendrite Development

If CD3ζ is a negative regulator of dendrite development, then activating endogenous protein should impair dendrite formation. We used a CD3ζ antibody targeted to the short extracellular domain of the molecule (antibody Ab22) as a tool that might potentially activate cell surface CD3ζ. Initial characterization of the intracellular signaling mediated by CD3ζ in leukocytes relied on the use of chimeric receptors comprising a heterologous cell-surface molecule fused to the cytoplasmic tail of CD3ζ (Irving and Weiss, 1991; Letourneur and Klausner, 1991). Application of antibodies to the cell surface of these chimeric receptors recapitulated the signal transduction events normally elicited by the intact TCR-CD3 receptor complex that leads to Ca^{2+} mobilization (Wange and Samelson, 1996). We applied a similar strategy with CD3ζ Ab22 antibody to measure Ca^{2+} mobilization by fluorescent Ca^{2+} imaging on live neurons. It is important to note that these experiments were carried out in the absence of the glial feeder layer, thus enabling measurement of direct effects of CD3ζ antibody on hippocampal neurons, because the low-density culture system we used represents a virtually pure neuron culture model (Goslin *et al.*, 1998). Experiments were performed in the absence of external Ca^{2+} to measure the release of Ca^{2+} from internal compartments. Application of 5 μg/ml control antibody (3g8) targeted to the extracellular sequence of the human transmembrane protein CD16 for 10 min did not affect the [Ca^{2+}]$_i$ level
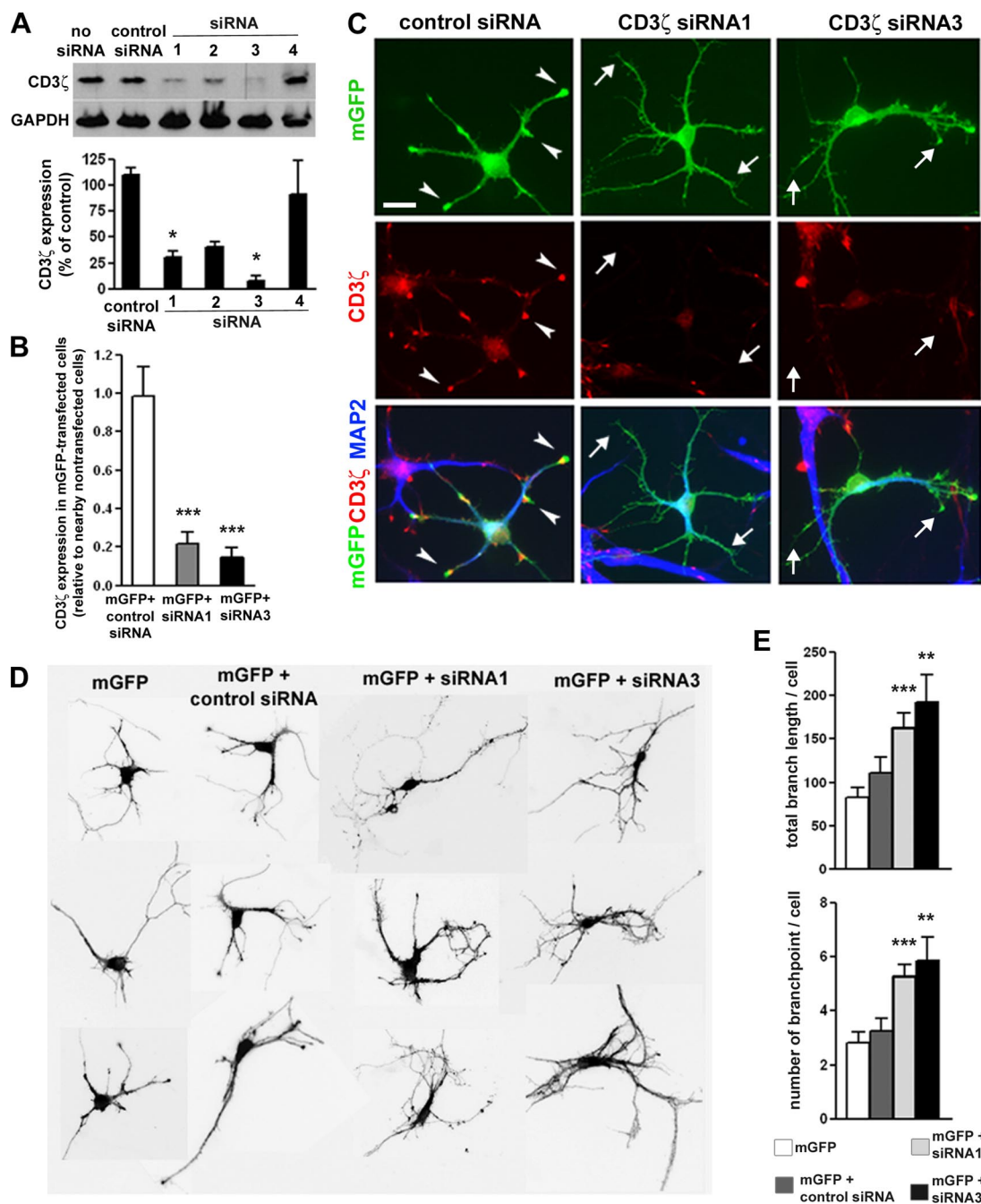
Figure 6. CD3ζ siRNA1 and siRNA3 promoted dendritic branching. (A) The efficacy and specificity of CD3ζ siRNA was tested in CD3ζ-transfected COS-7 cells by immunoblot analysis. An equal amount of protein was loaded for each lane, and the same samples were blotted against CD3ζ and GAPDH antibodies. CD3ζ siRNA1 and siRNA3 induced a strong suppression of CD3ζ expression. The signal intensity for each CD3ζ siRNA is plotted below as a percent of the signal intensity obtained from control CD3ζ-expressing COS-7 cells without siRNA. The data are expressed as mean ± SEM from four experiments (* $p < 0.05$ compared with cells transfected with CD3ζ plasmid alone). (B) Quantification of CD3ζ expression in cultured cortical neurons transfected at 3 DIV and immunostained at 5 DIV. Data are presented as a ratio of anti-CD3ζ fluorescence intensity in mGFP-positive cells relative to nearby nontransfected cells ± SEM (for each condition n > 15 cells from at least two cultures; *** $p < 0.001$). (C) Knockdown of neuronal CD3ζ expression by siRNA1 and siRNA3. Neurons were cotransfected at 3 DIV with mGFP (green) and either control siRNA or CD3ζ siRNA1 or siRNA3, and were immunolabeled at 5 DIV for CD3ζ (red) and the dendritic marker MAP2 (blue). Neurons transfected with a control siRNA show a robust CD3ζ immunoreactivity on dendrites (arrowheads). Neurons transfected with either CD3ζ siRNA1 or siRNA3 show a decreased CD3ζ immunoreactivity in dendrites (arrows) and a more complex dendritic arbor compared with control cells. (D) mGFP-labeled cultured cortical neurons transfected at 3 DIV and fixed at 5 DIV sampled from cultures transfected with mGFP alone, or mGFP + control siRNA, or mGFP + CD3ζ siRNA1, or mGFP + CD3ζ siRNA3. (E) Quantification of the total length and number of dendritic branches per cell. Data are presented as mean ± SEM of 29–63 cells from two to four independent cultures. ** $p < 0.01$, *** $p < 0.001$ (Student's *t* test) compared with corresponding measurements in cells cotransfected with mGFP and the control siRNA. Scale bar, 20 μm.
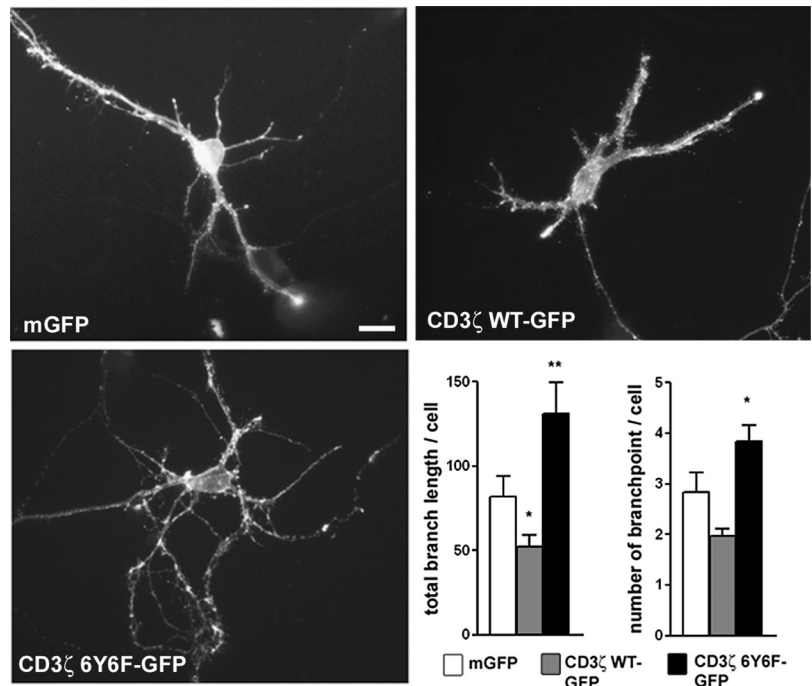
Figure 7. Overexpression of a CD3ζ mutant lacking the Tyr phosphorylation sites in the ITAMs increased dendritic branching. Neurons transfected at 3 DIV with mGFP or CD3ζ-GFP or CD3ζ-6Y6F-GFP were fixed at 5 DIV and were visualized by the GFP signal. The dendritic arborization was increased in neurons expressing CD3ζ-6Y6F-GFP but reduced in neurons expressing CD3ζ-GFP compared with control neurons transfected with mGFP. The length and number of dendritic branches were measured and data are expressed as the mean ± SEM of 32–58 cells from three independent experiments (bottom right). * p < 0.05 ,** p < 0.01 (Student's *t* test) compared with corresponding measurements in cells transfected with mGFP. Scale bar, 15 μm.

(Figure 8A). By contrast, the subsequent application of Ab22 CD3ζ antibody at 5 μg/ml onto the same cells induced a rapid rise of $[Ca^{2+}]_i$ in 87% of the neurons (46/53 recorded cells from three experiments; Figure 8A), indicating that CD3ζ Ab22 antibody induced a Ca^{2+} release from internal stores, likely through a direct binding to cell surface-associated CD3ζ proteins. These data suggest that Ab22 exhibits agonist-like activity and activates endogenous CD3ζ triggering a $[Ca^{2+}]_i$ increase. We thus applied CD3ζ Ab22 antibody to neuron culture to analyze the effects of endogenous CD3ζ recruitment on dendrite patterning. The CD3ζ antibody (5 μg/ml) was added at 1 and 3 DIV, and the cells were fixed at 5 DIV for MAP2 immunostaining followed by dendrite morphology analysis. The control cultures consisted in the addition of either the vehicle alone or the control antibody 3g8. No difference was observed in the dendritic arbor between the vehicle- and 3g8-treated neurons (for total branch length, vehicle-treated cells, 46.7 ± 7.6 μm, n = 52 cells, control antibody treated-cells, 52.0 ± 9.1 μm, n = 40 cells; p = 0.65; for branchpoint number, vehicle-treated cells, 1.71 ± 0.21, n = 52 cells control antibody treated-cells, 1.83 ± 0.23, n = 40 cells, p = 0.72; Figure 8, B and C). By contrast, substantial modifications of the dendritic profile were observed after CD3ζ Ab22 application. Both the total branch length and the number of branchpoints per cell were decreased by 78 and 67%, respectively, compared with control 3g8-treated cells (for total branch length per cell, 11.3 ± 2.3 μm, n = 50 cells, p < 0.001; for branchpoint number per cell, 0.60 ± 0.12, p < 0.001; Figure 8, B and C). Collectively, our data suggest that activating endogenous CD3ζ inhibits dendrite development in young neurons.

DISCUSSION

A novel idea is emerging that a large molecular repertoire is common to the nervous and immune systems, which might reflect the existence of neuronal functions for molecules originally characterized in the immune system. Alterna-

tively, such converging repertoire might also reflect physiological interactions between the two systems (Boulanger and Shatz, 2004; Steinman, 2004). Here, we show that the signaling adaptor protein CD3ζ, first described in the immune system (Samelson *et al.*, 1985), has a previously uncharacterized role in regulating neuronal development. CD3ζ distribution in developing neurons showed a selective association with dendritic filopodia and growth cones, actin-rich structures involved in neurite growth and patterning. Loss-of-function experiments by siRNA-mediated knockdown or by overexpression of CD3ζ mutated in its three ITAMs affected dendrite formation with an increased number and length of dendritic branching. Conversely, overexpressing CD3ζ or activating endogenous CD3ζ by a CD3ζ antibody reduced the length and number of dendritic branches. Altogether, our findings reveal a novel role for CD3ζ in the nervous system, highlighting its contribution to dendrite development through an ITAM-based mechanism.

Neuronal Expression of CD3ζ and Its Selective Association with Growth Cones and Filopodia in Young Neurons

We provide biochemical and immunohistochemical evidence for the expression of CD3ζ in the CNS. Previous studies reported the detection of CD3ζ mRNA in feline and mouse brain sections (Corriveau *et al.*, 1998; Huh *et al.*, 2000), but our study is the first to demonstrate expression of CD3ζ protein in brain slices and to identify the CD3ζ-expressing cells, which were predominantly neurons and to a lesser extent oligodendrocytes. The cellular distribution of CD3ζ immunoreactivity analyzed in developing hippocampal neurons showed a prominent enrichment at dendritic growth cones and filopodia in young neurons and at dendritic spines in mature neurons. These aforementioned neuronal subdomains are all actin-rich structures, and we indeed found in young neurons a striking colocalization of CD3ζ with F-actin. Treatment with the actin depolymerization agent cytochalasin D caused a dispersal of CD3ζ clus-
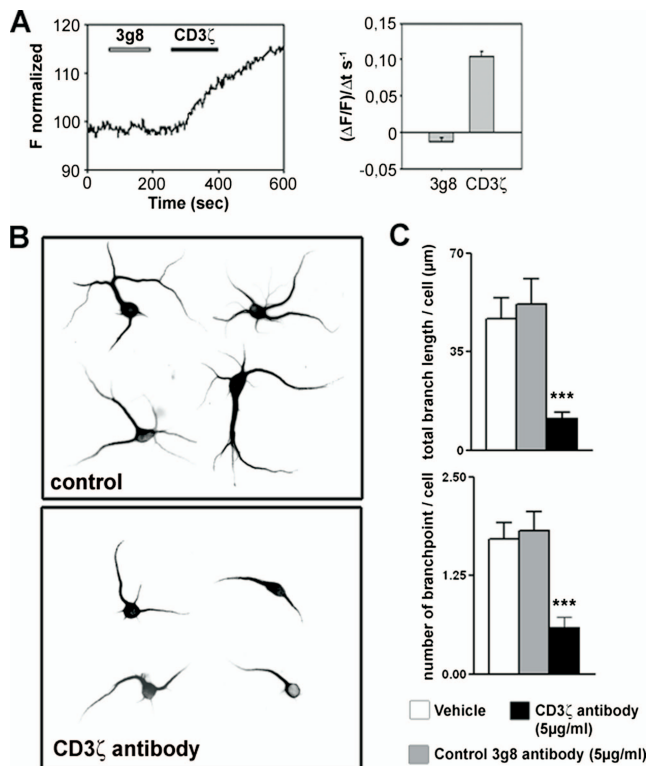
S. J. Baudouin *et al.*

Figure 8. Application of CD3ζ antibody to hippocampal cultured neurons induces an intracellular calcium increase and reduces the complexity of the dendritic arbor. (A) Cultured neurons at 7 DIV were loaded with Fluo-3 AM and exposed sequentially to the control antibody 3g8 (5 μg/ml) and to the CD3ζ Ab22 antibody (5 μg/ml). Left, representative relative fluo-3 fluorescence in response to 3g8 and CD3ζ antibodies shows a rise in $[Ca^{2+}]_i$ after CD3ζ antibody application. $[Ca^{2+}]_i$ increase was observed in 46 of 53 neurons from three different cultures. Right, bar graph comparing the slope of fluorescence increase triggered by 3g8 and CD3ζ antibodies. (B) MAP2-immunolabeled 5 DIV hippocampal neurons sampled from cultures treated with a control antibody (control) or with CD3ζ Ab22 antibody (CD3ζ antibody). (C) The length and number of dendritic branches were measured on neurons immunostained for MAP2. Results are shown as the mean ± SEM of 40–52 cells from two experiments. *** p < 0.001 (Student's *t* test) compared with corresponding measurements in 3g8 antibody-treated cells. Scale bar, 80 μm.

ters, indicating that the accumulation of CD3ζ at growth cones and filopodia was dependent on F-actin. Interestingly, CD3ζ remained colocalized with F-actin puncta spread throughout the neuropile upon actin disruption, suggesting a close molecular interaction between CD3ζ and F-actin. Association of CD3ζ with the actin cytoskeleton has been reported in lymphocytes and proposed to play a role in the dynamic rearrangements of the actin cytoskeleton required for the formation and stabilization of the immunological synapse at the interface between antigen-presenting cells and T lymphocytes (Caplan *et al.,* 1995; Rozdzial *et al.,* 1995; Krummel and Davis, 2002). In neurons, the localization of CD3ζ at cytoskeletal F-actin–rich structures positions it ideally for a role in the regulation of dendritic shaping driven by actin-based mechanisms. CD3ζ could directly bind actin filaments to regulate actin network assembly or act as an adaptor molecule that would connect membrane receptors and signaling proteins linked to the assembly/stability of actin cytoskeleton. In the latter case, one possibility is that

the effects of CD3ζ recruitment on neuronal morphogenesis involves the actin-related RhoA GTPase, which has been documented to inhibit dendritic growth and branch extension (Li *et al.,* 2000; Wong *et al.,* 2000).

Novel Function of CD3ζ in Dendrite Patterning
Our finding that CD3ζ was enriched at dendritic growth cones and filopodia in young neurons suggests a potential role for this molecule in dendrite morphogenesis. Accordingly, the inhibition of CD3ζ expression in cultured neurons by siRNA increased dendrite outgrowth, a phenotype similarly obtained by expression of a CD3ζ mutant lacking the Tyr phosphorylation sites within the ITAMs. The effects of the CD3ζ-6Y6F-GFP mutant were likely due to the competition with the endogenous protein and suggest that the role of CD3ζ on dendritic shaping required tyrosine-based signaling motifs. Conversely, CD3ζ overexpression, which presumably mimicked an increased recruitment of the protein, and CD3ζ antibody application, which acts through the activation of endogenously expressed CD3ζ, both reduced the length and number of dendritic branches. Together, these data suggest that CD3ζ acts as a negative regulator of dendritic arbor complexity through an ITAM-based mechanisms.

A critical role for CD3ζ in the establishment of the neuronal network has been described in the retinogeniculate projections of the visual system (Huh *et al.,* 2000). In mice lacking CD3ζ, the area of retinal projections in the lateral geniculate nucleus is abnormally larger and ectopic clusters of inputs were observed, indicating that CD3ζ is required to precisely restrict the field of retinal projections (Huh *et al.,* 2000). The fact that CD3ζ mRNA was detected in the lateral geniculate nucleus suggests a postsynaptic expression of CD3ζ proteins in this area (Huh *et al.,* 2000). In light of our results, one could hypothesize that CD3ζ deletion might result in an excessive dendritic arborization of lateral geniculate nucleus neurons, which in turn might induce a broader extension of axonal inputs, as observed in mutant mice.

Potential Mechanisms for CD3ζ Neuronal Function
In T-cell, CD3ζ is a component of the CD3 complex that also includes CD3ε, -γ, and -δ subunits. The CD3ε, -γ and -δ have all been detected in the cerebellum and CD3ε-deficient mice, in which CD3-γ and CD3-δ protein levels are also reduced, showed an impaired neuronal architecture of Purkinje neurons (Nakamura *et al.,* 2007). The cerebral expression of the four CD3 subunits raised the possibility that a kind of CD3 complex may exist in the brain similarly as in the immune system. However, CD3ζ mRNA was not detected in the cerebellum (Nakamura *et al.,* 2007), and we were not able to detect CD3ε at the protein level in forebrain samples (data not shown). Thus CD3ζ appeared to be expressed in distinct brain regions different from those for CD3ε, -γ, and -δ, suggesting that CD3ζ may function independently from the other CD3 subunits, as reported in NK cells (Lanier, 2001). One major issue that still needs to be resolved is the identification of the CD3ζ-bearing neuronal receptor, which could be either a known immune or neuronal receptor. Several CD3ζ-containing receptors have been identified in the immune system in both T-cells and NK cells. The most documented is the TCR in T-cells, which interacts with peptide-MHC complexes present on target cells (Samelson, 2002). The mRNA for the β subunit of the TCR has been detected in the murine CNS, but the absence of genomic recombination and the failure to detect the corresponding protein in brain homogenates make it unlikely to be the neuronal CD3ζ-containing receptor (Syken and Shatz, 2003; Nishiyori

et al., 2004). Other CD3ζ-containing receptors have been characterized in NK cells that belong to the family of activating receptors named NKp46, NKp30, and the low-affinity Fc receptor for IgG (Lanier, 2001). The neuronal expression of these NK cell–activating receptors has not been reported so far, and further studies will be required to identify the nature of the neuronal CD3ζ-associated receptor.

Also critical to understanding how CD3ζ control neuronal morphogenesis is identifying downstream signaling. We have found that mutagenesis of the three ITAMs reproduced the siRNA phenotype, suggesting that the function of CD3ζ in normal dendrite development was mediated through an ITAM-dependent mechanism. The current model of TCR-CD3 signaling in T-cells assumes that the ITAM phosphorylation of CD3ζ is a molecular switch that triggers the docking of SH2-containing signaling molecules such as the protein tyrosine kinases of the Syk/ZAP-70 family, which subsequently induces downstream signaling events including Ca^{2+} mobilization and activation of the Rho and Ras pathways (Pitcher and van Oers, 2003; Baniyash, 2004). In agreement with this, we found that CD3ζ recruitment by a CD3ζ antibody induced an elevation of $[Ca^{2+}]_i$ in cultured neurons. The expression of ZAP-70–related tyrosine kinase in developing neurons (Ishijima *et al.*, 1995; Yoneya *et al.*, 1998), and the reported role of Syk in neurite outgrowth (Tsujimura *et al.*, 2001; Gallagher *et al.*, 2007) is compatible with the notion that Syk/ZAP-70 could be a relevant component of the intracellular transduction pathway connecting CD3ζ activation and Ca^{2+} mobilization to negatively control dendritic shaping.

ACKNOWLEDGMENTS

REFERENCES

Baniyash, M. (2004). TCR zeta-chain downregulation: curtailing an excessive inflammatory immune response. Nat. Rev. Immunol. *4*, 675–687.

Barco, A., Patterson, S., Alarcon, J. M., Gromova, P., Mata-Roig, M., Morozov, A., and Kandel, E. R. (2005). Gene expression profiling of facilitated L-LTP in VP16-CREB mice reveals that BDNF is critical for the maintenance of LTP and its synaptic capture. Neuron *48*, 123–137.

Baudouin, S. J., Pujol, F., Nicot, A., Kitabgi, P., and Boudin, H. (2006). Dendrite-selective redistribution of the chemokine receptor CXCR4 following agonist stimulation. Mol. Cell Neurosci. *33*, 160–169.

Boulanger, L. M., and Shatz, C. J. (2004). Immune signalling in neural development, synaptic plasticity and disease. Nat. Rev. Neurosci. *5*, 521–531.

Caplan, S., Zeliger, S., Wang, L., and Baniyash, M. (1995). Cell-surface-expressed T-cell antigen-receptor zeta chain is associated with the cytoskeleton. Proc. Natl. Acad. Sci. USA *92*, 4768–4772.

Chan, A. C., Desai, D. M., and Weiss, A. (1994). The role of protein tyrosine kinases and protein tyrosine phosphatases in T cell antigen receptor signal transduction. Annu. Rev. Immunol. *12*, 555–592.

Corriveau, R. A., Huh, G. S., and Shatz, C. J. (1998). Regulation of class I MHC gene expression in the developing and mature CNS by neural activity. Neuron *21*, 505–520.

Dotti, C. G., Sullivan, C. A., and Banker, G. A. (1988). The establishment of polarity by hippocampal neurons in culture. J. Neurosci. *8*, 1454–1468.

Fink, C. C., Bayer, K. U., Myers, J. W., Ferrell, J. E., Jr., Schulman, H., and Meyer, T. (2003). Selective regulation of neurite extension and synapse formation by the beta but not the alpha isoform of CaMKII. Neuron *39*, 283–297.

Furukawa, T., Itoh, M., Krueger, N. X., Streuli, M., and Saito, H. (1994). Specific interaction of the CD45 protein-tyrosine phosphatase with tyrosine-phosphorylated CD3 zeta chain. Proc. Natl. Acad. Sci. USA *91*, 10928–10932.

Gallagher, D., Gutierrez, H., Gavalda, N., O'Keeffe, G., Hay, R., and Davies, A. M. (2007). Nuclear factor-kappaB activation via tyrosine phosphorylation of inhibitor kappaB-alpha is crucial for ciliary neurotrophic factor-promoted neurite growth from developing neurons. J. Neurosci. *27*, 9664–9669.

Garcia, G. G., and Miller, R. A. (1997). Differential tyrosine phosphorylation of zeta chain dimers in mouse CD4 T lymphocytes: effect of age. Cell Immunol. *175*, 51–57.

Geahlen, R. L., and McLaughlin, J. L. (1989). Piceatannol (3,4,3',5'-tetrahydroxy-trans-stilbene) is a naturally occurring protein-tyrosine kinase inhibitor. Biochem. Biophys. Res. Commun. *165*, 241–245.

Goslin, K., Asmussen, H., and Banker, G. (1998). Rat hippocampal neurons in low density culture. In: Culturing Nerve Cells, ed. G. Banker and K. Goslin, Cambridge, MA: MIT Press, 339–370.

Huh, G. S., Boulanger, L. M., Du, H., Riquelme, P. A., Brotz, T. M., and Shatz, C. J. (2000). Functional requirement for class I MHC in CNS development and plasticity. Science *290*, 2155–2159.

Irving, B. A., and Weiss, A. (1991). The cytoplasmic domain of the T cell receptor zeta chain is sufficient to couple to receptor-associated signal transduction pathways. Cell *64*, 891–901.

Ishijima, S. A., Zeng, Y. X., Kurashima, C., Utsuyama, M., Shirasawa, T., Sakamoto, K., and Hirokawa, K. (1995). Expression of ZAP-70 gene in the developing thymus and various nonlymphoid tissues of embryonic and adult mice. Cell Immunol. *165*, 278–283.

Itoh, Y., Matsuura, A., Kinebuchi, M., Honda, R., Takayama, S., Ichimiya, S., Kon, S., and Kikuchi, K. (1993). Structural analysis of the CD3 zeta/eta locus of the rat. Expression of zeta but not eta transcripts by rat T cells. J. Immunol. *151*, 4705–4717.

Jaworski, J., Spangler, S., Seeburg, D. P., Hoogenraad, C. C., and Sheng, M. (2005). Control of dendritic arborization by the phosphoinositide-3'-kinase-Akt-mammalian target of rapamycin pathway. J. Neurosci. *25*, 11300–11312.

Krummel, M. F., and Davis, M. M. (2002). Dynamics of the immunological synapse: finding, establishing and solidifying a connection. Curr. Opin. Immunol. *14*, 66–74.

Kumanogoh, A., and Kikutani, H. (2003). Immune semaphorins: a new area of semaphorin research. J. Cell Sci. *116*, 3463–3470.

Lanier, L. L. (2001). On guard—activating NK cell receptors. Nat. Immunol. *2*, 23–27.

Letourneur, F., and Klausner, R. D. (1991). T-cell and basophil activation through the cytoplasmic tail of T-cell-receptor zeta family proteins. Proc. Natl. Acad. Sci. USA *88*, 8905–8909.

Li, Z., Van Aelst, L., and Cline, H. T. (2000). Rho GTPases regulate distinct aspects of dendritic arbor growth in *Xenopus* central neurons in vivo. Nat. Neurosci. *3*, 217–225.

Lohmann, C., Myhr, K. L., and Wong, R. O. (2002). Transmitter-evoked local calcium release stabilizes developing dendrites. Nature *418*, 177–181.

Lowin-Kropf, B., Shapiro, V. S., and Weiss, A. (1998). Cytoskeletal polarization of T cells is regulated by an immunoreceptor tyrosine-based activation motif-dependent mechanism. J. Cell Biol. *140*, 861–871.

Mahanthappa, N. K., and Patterson, P. H. (1992). Thy-1 involvement in neurite outgrowth: perturbation by antibodies, phospholipase C, and mutation. Dev. Biol. *150*, 47–59.

Malissen, M. *et al.* (1993). T cell development in mice lacking the CD3-zeta/eta gene. EMBO J. *12*, 4347–4355.

Moriyoshi, K., Richards, L. J., Akazawa, C., O'Leary, D. D., and Nakanishi, S. (1996). Labeling neural cells using adenoviral gene transfer of membrane-targeted GFP. Neuron *16*, 255–260.

Morris, R. (1985). Thy-1 in developing nervous tissue. Dev. Neurosci. *7*, 133–160.

Nakamura, K. *et al.* (2007). CD3 and immunoglobulin G Fc receptor regulate cerebellar functions. Mol. Cell. Biol. *27*, 5128–5134.

Nishiyori, A., Hanno, Y., Saito, M., and Yoshihara, Y. (2004). Aberrant transcription of unrearranged T-cell receptor beta gene in mouse brain. J. Comp. Neurol. *469*, 214–226.

Pitcher, L. A., and van Oers, N. S. (2003). T-cell receptor signal transmission: who gives an ITAM? Trends Immunol. *24*, 554–560.

Polleux, F., Morrow, T., and Ghosh, A. (2000). Semaphorin 3A is a chemoattractant for cortical apical dendrites. Nature *404*, 567–573.

Pujol, F., Kitabgi, P., and Boudin, H. (2005). The chemokine SDF-1 differentially regulates axonal elongation and branching in hippocampal neurons. J. Cell Sci. *118*, 1071–1080.

Reynolds, B. A., Tetzlaff, W., and Weiss, S. (1992). A multipotent EGF-responsive striatal embryonic progenitor cell produces neurons and astrocytes. J. Neurosci. *12*, 4565–4574.

Rozdzial, M. M., Malissen, B., and Finkel, T. H. (1995). Tyrosine-phosphorylated T cell receptor zeta chain associates with the actin cytoskeleton upon activation of mature T lymphocytes. Immunity *3*, 623–633.

Samelson, L. E. (2002). Signal transduction mediated by the T cell antigen receptor: the role of adapter proteins. Annu. Rev. Immunol. *20*, 371–394.

Samelson, L. E., Harford, J. B., and Klausner, R. D. (1985). Identification of the components of the murine T cell antigen receptor complex. Cell *43*, 223–231.

Sancho, J., Peter, M. E., Franco, R., Danielian, S., Kang, J. S., Fagard, R., Woods, J., Reed, J. C., Kamoun, M., and Terhorst, C. (1993). Coupling of GTP-binding to the T cell receptor (TCR) zeta-chain with TCR-mediated signal transduction. J. Immunol. *150*, 3230–3242.

Sergent-Tanguy, S., Veziers, J., Bonnamain, V., Boudin, H., Neveu, I., and Naveilhan, P. (2006). Cell surface antigens on rat neural progenitors and characterization of the CD3 (+)/CD3 (−) cell populations. Differentiation *74*, 530–541.

Sourial-Bassillious, N., Eklof, A. C., Scott, L., Aperia, A., and Zelenin, S. (2006). Effect of TNF-alpha on CD3-zeta and MHC-I in postnatal rat hippocampus. Pediatr. Res. *60*, 377–381.

Steinman, L. (2004). Elaborate interactions between the immune and nervous systems. Nat. Immunol. *5*, 575–581.

Syken, J., and Shatz, C. J. (2003). Expression of T cell receptor beta locus in central nervous system neurons. Proc. Natl. Acad. Sci. USA *100*, 13048–13053.

Terry-Lorenzo, R. T., Roadcap, D. W., Otsuka, T., Blanpied, T. A., Zamorano, P. L., Garner, C. C., Shenolikar, S., and Ehlers, M. D. (2005). Neurabin/protein phosphatase-1 complex regulates dendritic spine morphogenesis and maturation. Mol. Biol. Cell *16*, 2349–2362.

Tsujimura, T., Yanagi, S., Inatome, R., Takano, T., Ishihara, I., Mitsui, N., Takahashi, S., and Yamamura, H. (2001). Syk protein-tyrosine kinase is involved in neuron-like differentiation of embryonal carcinoma P19 cells. FEBS Lett. *489*, 129–133.

van Oers, N. S., Tohlen, B., Malissen, B., Moomaw, C. R., Afendis, S., and Slaughter, C. A. (2000). The 21- and 23-kD forms of TCR zeta are generated by specific ITAM phosphorylations. Nat. Immunol. *1*, 322–328.

Wange, R. L., and Samelson, L. E. (1996). Complex complexes: signaling at the TCR. Immunity *5*, 197–205.

Whitford, K. L., Marillat, V., Stein, E., Goodman, C. S., Tessier-Lavigne, M., Chedotal, A., and Ghosh, A. (2002). Regulation of cortical dendrite development by Slit-Robo interactions. Neuron *33*, 47–61.

Wong, W. T., Faulkner-Jones, B. E., Sanes, J. R., and Wong, R. O. (2000). Rapid dendritic remodeling in the developing retina: dependence on neurotransmission and reciprocal regulation by Rac and Rho. J. Neurosci. *20*, 5024–5036.

Wu, J. Y., Feng, L., Park, H. T., Havlioglu, N., Wen, L., Tang, H., Bacon, K. B., Jiang, Z., Zhang, X., and Rao, Y. (2001). The neuronal repellent Slit inhibits leukocyte chemotaxis induced by chemotactic factors. Nature *410*, 948–952.

Yoneya, H., Yanagi, S., Inatome, R., Ding, J., Hitomi, T., Amatsu, M., and Yamamura, H. (1998). Antibodies directed against ZAP-70 cross-react with a 66-kDa tyrosine kinase in the rat brain. Biochem. Biophys. Res. Commun. *245*, 140–143.